

## Quantum Superposition of High Spin States in the Single Molecule Magnet Ni<sub>4</sub>

E. del Barco,<sup>1</sup> A. D. Kent,<sup>1</sup> E. C. Yang,<sup>2</sup> and D. N. Hendrickson<sup>2</sup>

<sup>1</sup>*Department of Physics, New York University, 4 Washington Place, New York, New York 10003, USA*

<sup>2</sup>*Department of Chemistry and Biochemistry, University of California San Diego, La Jolla, California 92093-0358, USA*

(Received 14 May 2004; published 4 October 2004)

Quantum tunneling of the magnetization in a single molecule magnet has been studied in experiments that combine microwave spectroscopy with high sensitivity magnetic measurements. By monitoring spin-state populations in the presence of microwave radiation, the energy splittings between low lying superpositions of high-spin states of single molecule magnet Ni<sub>4</sub> ( $S = 4$ ) have been measured. Absorption linewidths give an upper bound on the rate of decoherence. Pulsed microwave experiments provide a measure of energy relaxation time, which is found to increase with frequency.

DOI: 10.1103/PhysRevLett.93.157202

PACS numbers: 75.50.Tt, 75.45.+j, 75.60.Lr

Quantum tunneling of the magnetization (QTM) in single molecule magnets (SMMs) enables the creation of superpositions of high-spin states, which are both of great fundamental interest and essential for the use of SMMs in quantum computing [1,2]. The main focus of experiments conducted to date, however, have been on incoherent QTM, where these superposition states are subject to rapid decay into their classical counterparts: spin-up and spin-down states [3–5]. Decoherence generally occurs when discrete levels are coupled to an environment with many degrees of freedom, such as the modes of a lattice (phonons), the electromagnetic field (photons) or nuclear spins [6–8]. Here we investigate coherent QTM in a SMM in which the tunneling rate is faster than the rate of decoherence and at a temperature at which tunneling occurs only between the lowest lying spin states. Our experiments combine microwave excitations with high sensitivity magnetic measurements [9] and enable continuous monitoring of spin-state populations during the application of pulsed and continuous microwave radiation. The linewidths associated with microwave absorption provide an upper bound on the decoherence rate of the superposition of high-spin states in a SMM.

We have chosen to study [Ni(hmp)(*t*-BuEtOH)Cl]<sub>4</sub>, henceforth referred to as Ni<sub>4</sub>, because this is a particularly clean SMM, with no nuclear spins on the transition metal sites [10]. The molecule core consists of four Ni<sup>II</sup> (spin 1) magnetic ions and oxygen atoms at alternating corners of a distorted cube, with  $S_4$  site symmetry. Ferromagnetic exchange interactions between the Ni<sup>II</sup> ions lead to an  $S = 4$  ground state at low temperature, as determined by magnetic susceptibility and high frequency electron paramagnetic resonance (EPR) measurements [10]. Magnetic hysteresis is observed below a characteristic blocking temperature (1 K) and is associated with the presence of a uniaxial magnetic anisotropy that favors high-spin projections on the easy axis of the molecule, which we denote the  $z$  axis. This uniaxial anisotropy leads to large energy barrier ( $DS^2 \sim 12$  K) to magnetization reversal.

QTM is characterized by the spin Hamiltonian:

$$\mathcal{H} = -DS_z^2 - \mu_B \vec{S} \cdot \hat{g} \cdot \vec{H}, \quad (1)$$

where the first term is the uniaxial anisotropy and the second term is the Zeeman energy. An external magnetic field applied along the easy axis of the molecules  $H_z$ , tilts the double potential well favoring those spin projections aligned with the field. Note that in zero magnetic field the  $|\text{up}\rangle$  and  $|\text{down}\rangle$  spin projections have nearly the same energy and QTM is possible. Importantly, in this case, a magnetic field transverse to the anisotropy axis (in the  $x$ - $y$  plane) lifts the degeneracy of these states by an energy  $\Delta$ , the tunnel splitting, and leads to states that are superpositions of the original  $|\text{up}\rangle$  and  $|\text{down}\rangle$  spin projections [Fig. 1(a)]. The frequency of QTM between  $|\text{up}\rangle$  and  $|\text{down}\rangle$  states is proportional to the tunnel splitting ( $f = \Delta/h$ ). In the presence of a transverse field the states are superpositions of opposite spin projections

$$\begin{aligned} |S\rangle &= \frac{1}{\sqrt{2}}(|\text{up}\rangle + |\text{down}\rangle), \\ |A\rangle &= \frac{1}{\sqrt{2}}(|\text{up}\rangle - |\text{down}\rangle), \end{aligned} \quad (2)$$

where

$$\begin{aligned} |\text{up}\rangle &= \frac{1}{\sqrt{2}} \sum_m (a_m + b_m) |m\rangle, \\ |\text{down}\rangle &= -\frac{1}{\sqrt{2}} \sum_m (a_m - b_m) |m\rangle. \end{aligned} \quad (3)$$

The value of the coefficients  $a_m$  and  $b_m$  depend on the applied field. As an example, for small transverse fields ( $H_T \rightarrow 0$ ), the two lowest levels are approximately given by  $|S\rangle = (1/\sqrt{2})(|+4\rangle + |-4\rangle)$  and  $|A\rangle = (1/\sqrt{2})(|+4\rangle - |-4\rangle)$ . In the presence of a large transverse magnetic field the  $|\text{up}\rangle$  and  $|\text{down}\rangle$  states are tilted away from the  $z$  axis but still separated by a large angle when this field is less than the anisotropy field  $H_a = 2DS/(g\mu_B) = 4.5$  T.

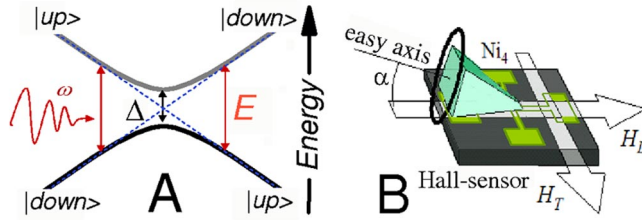


FIG. 1 (color online). (a) Energy of the lowest lying  $\text{Ni}_4$  levels,  $|S\rangle$  and  $|A\rangle$ , in the vicinity of zero longitudinal field, in the presence of a transverse field. (b) Experimental configuration.

The interaction of the spin with the environment limits the coherence time of the superposition. A transverse field can be used to increase the tunnel splitting and access a regime in which the dynamics is expected to be coherent [7,8]. It is straightforward to show that the tunnel splitting depends on the transverse field to a high power,  $\sim D(H_T/H_a)^{2S}$  [11]. This enables large variations in the magnitude of the tunnel splitting for small changes in the transverse field. Photon induced transitions (PIT) between symmetric and antisymmetric states produce changes of the  $z$  component of magnetization when the longitudinal field is nonzero. When the microwave field,  $H_{ac}$ , is parallel to the easy axis the transition rate is given by the following expression:

$$\Gamma = \frac{\pi}{2} \left( \frac{g\mu_B}{\hbar} H_{ac} \right)^2 |\langle S|S_z|A\rangle|^2 f(\omega), \quad (4)$$

where  $\langle S|S_z|A\rangle$  is the matrix element coupling the symmetric and antisymmetric states.  $f(\omega)$  is a Lorentzian which characterizes the linewidth of the resonance

$$f(\omega) = \frac{1}{\pi} \frac{\tau_2}{1 + (\omega - \omega_0)^2 \tau_2^2}, \quad (5)$$

where  $\omega_0 = E/\hbar$ , and  $E \approx \sqrt{(g\mu_B S_z H_z)^2 + \Delta^2}$  is the energy level separation.  $\tau_2$  is the transverse relaxation time, which sets the width of the resonance. Note that the transition matrix element is maximum at zero longitudinal magnetic field, when the states are symmetric and antisymmetric superpositions of  $|up\rangle$  and  $|down\rangle$  states. The matrix element decreases with longitudinal magnetic field and approaches zero when  $2g\mu_B H_z \gg \Delta$ , and states are simple up and down spin projections.

We have conducted experiments in a low temperature limit,  $k_B T < E$ , in which there is a significant difference in the population between the two lowest lying spin levels. A high sensitivity micro-Hall effect magnetometer is used to measure the magnetization of a millimeter-sized single crystal (pyramidal shape) of  $\text{Ni}_4$  that is placed with one of its faces parallel to the plane of the Hall sensor [12] [see Fig. 1(b)]. The  $z$  axis, which is parallel to the axis of the pyramid, is misaligned with respect to the plane of the sensor by  $\alpha = 20^\circ$ . The Hall device responds to the

average magnetic field perpendicular to the plane of the sensor [13], which for the sample shape and placement, is mainly due to the  $z$  component of sample magnetization. The experiments were conducted at 0.38 K in a  $\text{He}^3$  cryostat (sample in vacuum) that incorporates a 3D vector superconducting magnet, in which magnetic fields can be applied in arbitrary directions with respect to the axes of a crystal. A thin circular superconducting loop ( $\phi = 2$  mm) is placed with its plane perpendicular to the easy anisotropy axis of the crystal [see Fig. 1(b)]. This loop shorts the end of a 2.4 mm coaxial line. All the measurements were performed at loop resonances to maximize the microwave power that is converted into ac magnetic field at the sample position. Further, pulsed microwave experiments were conducted using a pulse pattern generator to gate the microwave source.

Figure 2(a) shows a magnetization curve recorded in the presence of continuous-wave (cw) radiation at 39.8 GHz while a transverse field of 3.2 T was applied [14]. Peaks and dips are observed at opposite polarities of the longitudinal field demonstrating PITs between magnetic states of the molecules with opposite spin projections. At PITs the sample temperature increases by less than 0.01 K (measured with a thermometer placed close to the sample), showing that these features are not due to

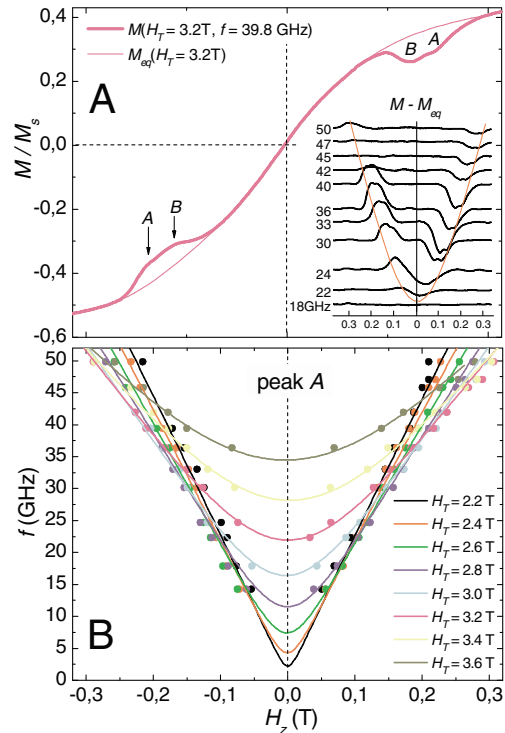


FIG. 2 (color online). (a)  $M$  vs  $H_z$  in the presence of a transverse field,  $H_T = 3.2$  T, while cw radiation of 39.8 GHz was applied ( $P_{\text{source}} = 2$  dBm). The inset shows  $M - M_{\text{eq}}$  versus longitudinal field at different microwave frequencies. (b) Field positions of the PITs of species A for several microwave frequencies and transverse fields.

sample heating ( $\Delta T \approx 1$  K would be necessary to explain the observed changes). A careful inspection of the peaks shows a more complex structure: each peak is formed by two peaks, labeled *A* and *B*. Measurements carried out at lower sweep rates show that peak *B* is also composed of two peaks,  $B_1$  and  $B_2$  (see Figs. 3 and 4). This is in agreement with longitudinal field EPR experiments, where different absorption lines have been found and ascribed to molecules with slightly different values of the axial anisotropy parameter [15].

Classically the energy of these states would depend linearly on magnetic field and simply cross at zero field. However, the position of the peaks as a function of frequency does not depend linearly on magnetic field, particularly near zero longitudinal field. This is evident in Fig. 2(b), which shows the position of peak *A* versus  $H_z$  at different frequencies and as a function of the transverse field (2.2 to 3.6 T). The curvature of the energy splitting as the longitudinal field goes to zero is evidence of level repulsion and, with the measured magnetization changes, is a *clear signature of quantum superposition states with opposite magnetization*. The solid lines are fits of the data by direct diagonalization of the Hamiltonian of Eq. (1) using  $D_A = 0.765$  K,  $B = 7.9 \times 10^{-3}$  K,  $C = 3.25 \times 10^{-5}$  K,  $g_z = 2.3$ ,  $g_x = g_y = 2.23$  [16]. The behavior of the *B* peaks can be fit with parameters  $D_{B1} = 0.735$  and  $D_{B2} = 0.745$  K (not shown). These values are in excellent agreement with those determined from high frequency EPR experiments [15].

We have measured the change in magnetic response as a function of the power of the incident cw radiation

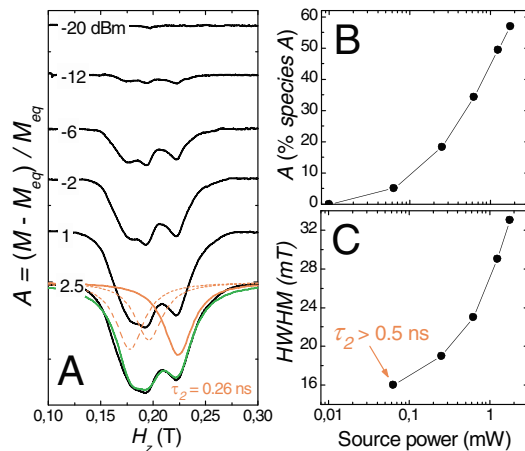


FIG. 3 (color online). (a)  $(M - M_{eq})/M_{eq}$  for different powers with cw 39.4 GHz radiation applied to the sample. The longitudinal field was swept at  $1.6 \times 10^{-4}$  T/s and  $H_T = 3.2$  T. The curves are offset for clarity. The green line is a fit to the sum of three Lorentzian functions. The red lines are the Lorentzian functions corresponding to dip *A* (solid) with  $\tau_2 = 0.26$  ns and dips  $B_1$  and  $B_2$  (dashed), for  $P_{source} = 2.5$  dBm. (b), (c) show the dependence of the amplitude and half width of PIT *A* as a function of the source power, respectively.

(39.4 GHz) to estimate the decoherence rate. A transverse magnetic field of 3.2 T is applied and a longitudinal field is swept at a rate of  $1.6 \times 10^{-4}$  T/s. The microwave power at the source was varied from  $-20$  to 2.5 dBm [17]. The normalized change in magnetization  $(M - M_{eq})/M_{eq}$  is shown as a function of the longitudinal field in Fig. 3(a) for different microwave powers. We have fit the results shown in Fig. 4(a) to a multipole Lorentzian function,  $f_T(\omega) = \sum f_i(\omega)$  ( $i = 1, 2, 3$ ). We find that  $\tau_2 = 0.26$  ns from the width of PIT *A* of the curve measured with  $P_{source} = 2.5$  dBm, or a resonance quality factor  $Q \sim 10$ . In Fig. 3(c) we show the dependence of PIT *A*'s half width at half maximum (HWHM) versus the microwave power at the source. The minimum width (lowest power) gives  $\tau_2 = 0.5$  ns, which can be considered as a lower bound for the decoherence time,  $\tau_\phi > 0.5$  ns. A very similar lower bound of the decoherence time,  $\tau_\phi > 1$  ns, has been recently reported in high frequency EPR experiments carried out in a single crystal of a  $Mn_4$  SMM dimer ( $S = 9/2$ ) [18].

In order to study the dynamics of the magnetization in the presence of radiation, we have conducted experiments with pulsed microwave radiation, in which the pulse time is of the order of the energy relaxation time ( $\sim$  sec). We sweep the applied longitudinal field at a rate of  $8.3 \times 10^{-5}$  T/s, with  $H_T = 3.2$  T, around the position of a PIT, while the magnetization is continuously

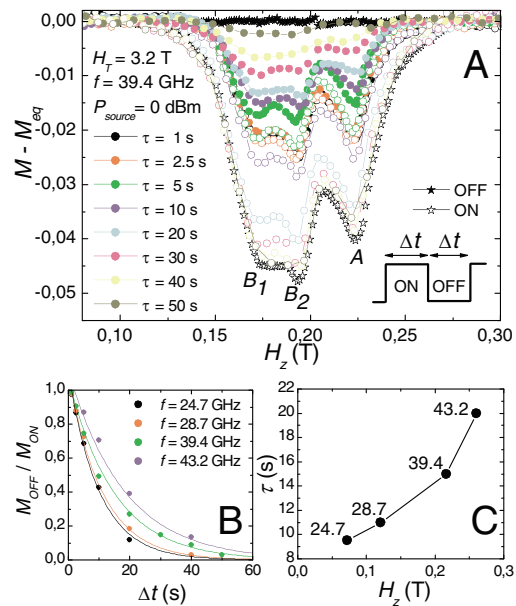


FIG. 4 (color online). (a) Boundaries  $M_{ON}$  (open circles) and  $M_{OFF}$  (solid circles) of the magnetization in a pulsed microwave experiment. The black curves were measured with 99.99% (open black stars) and 0.01% (solid black stars) duty cycles. (b) The ratio between  $M_{OFF}$  and  $M_{ON}$  for PIT *A* versus pulse width for four different frequencies. The lines are fits to an exponential decay with a characteristic time  $\tau$ . (c)  $\tau$  as a function of the longitudinal field.

monitored. During this field sweep we apply pulses of 39.4 GHz with a 50% duty cycle and pulse times,  $\Delta t$ , from 1 to 50 s. The maxima and minima in the magnetization, which occur at the end of the on and off pulses (labeled ON and OFF, respectively), are plotted versus the applied field in Fig. 4(a). We note that due to heating of the sample and sensor  $M_{\text{ON}}$  is shifted from  $M_{\text{OFF}}$  for pulse widths greater than 1 sec even for longitudinal magnetic fields away from the PIT dip. For this reason the curves for  $M_{\text{ON}}$  have been shifted to coincide with  $M_{\text{OFF}}$  curves away from the PIT dip, with all curves displaced by the same amount independent of the pulse width. The temperature change between on and off pulses is also field independent ( $\sim 0.1$  K). The ratio  $M_{\text{OFF}}/M_{\text{ON}}$  is found to depend exponentially on the pulse width  $M_{\text{OFF}}/M_{\text{ON}} = \exp(-\Delta t/\tau)$  [19]. A fit to this expression gives  $\tau$ , the energy relaxation time. We have repeated this experiment for frequencies between 24.7 and 43.2 GHz at the same transverse field [Fig. 4(b)].  $\tau$  is plotted as a function of longitudinal field in Fig. 4(c). The relaxation time increases from 8 to 20 s as the field and thus frequency increases. This may indicate a long spin-lattice relaxation time. However, we cannot exclude the possibility that this reflects the thermal coupling between the sample and bath or changes in the radiation power as a function of frequency [20]. Experiments with different sample sizes, radiation frequencies and powers are necessary for a more detailed understanding of this relaxation phenomena.

More importantly, this experiment places bounds on the decoherence time, which is the critical parameter for the implementation of SMMs in quantum computation [2]. The width of the absorption line [represented by  $\tau_2$  in Eq. (5)] is usually taken as a lower bound for the decoherence time. However, if the linewidth is associated with inhomogeneous broadening, such as by dipolar and hyperfine fields (from the many atoms with nuclear moments in the molecule) the coherence time could be significantly longer. We note increasing the coherence is very likely to be amenable to synthetic strategies of nuclear isotope purification and further reduction of intermolecular interactions. These will be the subject of future investigations along with studies of Rabi oscillations in molecular nanomagnets induced by shorter and higher amplitude pulsed microwave magnetic fields.

This research was supported by NSF (Grants No. DMR-0103290, No. 0114142, and No. 0315609).

- 
- [1] A. J. Leggett, Prog. Theor. Phys. Suppl. **69**, 80 (1980).
  - [2] M. Leuenberger and D. Loss, Nature (London) **410**, 789 (2001).
  - [3] J. R. Friedman *et al.*, Phys. Rev. Lett. **76**, 3830 (1996); J. M. Hernandez *et al.*, Europhys. Lett. **35**, 301 (1996); L. Thomas *et al.*, Nature (London) **383**, 145 (1996).

- [4] W. Wernsdorfer and R. Sessoli, Science **284**, 133 (1999).
- [5] L. Sorace *et al.*, Phys. Rev. B **68**, 220407(R) (2003).
- [6] N. V. Prokof'ev and P. C. E. Stamp, Rep. Prog. Phys. **63**, 669 (2000).
- [7] P. C. E. Stamp and I. S. Tupitsyn, Phys. Rev. B **69**, 014401 (2004).
- [8] E. M. Chudnovsky, Phys. Rev. Lett. **92**, 120405 (2004).
- [9] See also, W. Wernsdorfer, A. Müller, D. Mailly, and B. Barbara, Europhys. Lett. **66**, 861 (2004).
- [10] E. C. Yang *et al.*, Polyhedron **22**, 1727 (2003).
- [11] D. A. Garanin and E. M. Chudnovsky, Phys. Rev. B **56**, 11102 (1997).
- [12] A. D. Kent, S. von Molnar, S. Gider and D. D. Awschalom, J. Appl. Phys. **76**, 6656 (1994).
- [13] See, for example, S. Liu, H. Guillou, A. D. Kent, G. W. Stupian, and M. S. Leung, J. Appl. Phys. **83**, 6161 (1998).
- [14] The total transverse field felt by the molecules varies slightly with  $H_L$  due to a second misalignment between the  $z$  axis and the projection of  $H_L$  on the sensor plane,  $\theta = 5.3^\circ$ . This variation ( $H_x = H_T \cos\theta + H_L \cos\alpha \sin\theta$ ) leads to small asymmetries in both the position and magnitude of the peaks/dips seen in Figs. 2(a) and 2(b), where the data is plotted as a function of  $H_z = H_L \cos\alpha \cos\theta + H_T \sin\theta$ .
- [15] R. S. Edwards *et al.*, J. Appl. Phys. **93**, 7807 (2003).
- [16] There is an additional transverse anisotropy term in Eq. (1) of the form  $C(S_+^4 + S_-^4)$  seen in EPR studies [10,15].
- [17] Considering the losses in the coaxial line ( $\sim 15$  dB) and the measured reflected power ( $-55$  dB), we estimate that the power irradiated by the loop antenna is  $P_{\text{loop}} = 0.032P_{\text{source}}$ . Taking into account the change in the magnetization at the PIT, we estimate that the power absorbed by the sample is 2% of the power irradiated by the loop antenna. So for the highest power in Fig. 3(a) (39.4 GHz), the power absorbed is  $\sim 1 \mu\text{W}$ .
- [18] S. Hill, R. S. Edwards, N. Aliaga-Alcalde, and G. Christou, Science **302**, 1015 (2003).
- [19] This analysis is valid for exponential relaxation of non-interacting magnets. In this case the relaxation rate is independent of the normalization. However, if interactions are important then the relaxation will depend on the initial magnetization state. Since in these experiments, the initial magnetization,  $M_{\text{ON}}$ , depends on the pulse width, our analysis would not properly describe collective relaxation phenomena.
- [20] The radiation power for frequencies below 37 GHz has been chosen to maintain the sample at 0.50 K. However, for the higher frequency data of Fig. 3 the maximum power available lead to a sample temperature of 0.45 K. Therefore, the relaxation times for 39.4 and 43.2 GHz are determined under conditions of slightly different (lower) microwave power. Experiments carried out at constant microwave power and faster field sweep rates lead to an asymmetric broadening of the PITs that clearly indicates that the relaxation time increases with longitudinal field and thus with frequency (to be published).